

THE INFLUENCE OF LARGE-SCALE SOIL MOISTURE HETEROGENEITY ON WETTING AND DRYING PLANETARY BOUNDARY LAYERS

Edward G. Patton*, Peter P. Sullivan and Chin-Hoh Moeng
National Center for Atmospheric Research, Boulder, CO

1. INTRODUCTION

Land-atmosphere coupling is widely recognized as a crucial component of regional, continental and global scale numerical models. Predictions from these large-scale models are sensitive to small scale surface layer processes like heat and moisture fluxes at the air-soil-vegetation interface as well as boundary layer treatments (*e.g.*, Garratt, 1993). The soil moisture boundary condition has a considerable influence on medium-to-long range weather forecasts and on simulated monthly mean climatic states (*e.g.*, Rowntree and Bolton, 1983). The resolution used in most large scale models is however relatively coarse so that the turbulent processes in the planetary boundary layer (PBL) which control the surface fluxes are not resolved but are determined by a parameterization. In our view, the shortcomings and sensitivities exhibited by large scale numerical models are partly a consequence of inadequate modeling of the PBL and its interaction with the land surface. In order to improve existing parameterizations, a more complete understanding of the mechanics and thermodynamics of air-soil interaction and the transport of water vapor by turbulent processes in the PBL is required.

There have been a few prior investigations into the effects of non-homogeneous surface forcing on the PBL using LES (*e.g.*, Roy and Avissar, 2000; Shen and Leclerc, 1995). Typically in these studies the surface fluxes are prescribed and relatively coarse grid resolution is used. In the work described here, the interactions between land surfaces and the atmosphere are examined by coupling a large-eddy simulation (LES) model for the PBL to a land surface model (LSM). Fine grids and large computational domains are used to examine the impact of large scale soil moisture heterogeneity on PBL turbulence and the vertical flux of water vapor mixing ratio. The heterogeneity is shown to influence the PBL differently depending on the moisture content of the overlying air.

*corresponding author address: Edward G. Patton, National Center for Atmospheric Research, P. O. Box 3000, Boulder, CO 80307-3000; email: ned@patton.net

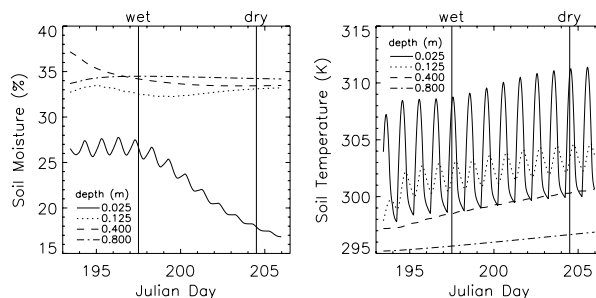


Figure 1: Time evolution of the four vertical levels of soil moisture and temperature from the 1-D off-line LSM run initialized from measurements from Little Washita at 11:30am local time on Day 193 of SGP97. Initial conditions for the LSM for the *wet* and *dry* coupled simulations are taken at noon seven days apart.

2. Land-Atmosphere Coupling

We use our well established 3D, time-dependent, LES code as the parent atmospheric model (see Sullivan et al., 1996, for a description of the code and further references). Numerous models of varying sophistication and empirical content have been proposed to describe the physics of soil-water-vegetation systems. For our coupling studies, we have adopted the so called NOAH (National Center for Environmental Prediction / Oregon State University / Air Force / Office of Hydrology) LSM, version 2.0. The NOAH LSM is used in several large scale atmospheric models and has been validated against observations (Chang et al., 1999).

3. The LSM: Deployment, Input Parameters, and Initial Conditions

The LSM is implemented at every x,y grid point in the LES. Each of these grid points is covered by perennial grasses, with a surface roughness for momentum z_{om} of 0.1 m, and overlays four silty clay loam soil layers at depths of [0.05,0.20,0.60,1.00] m. A surface albedo of 0.2 is used.

Initial soil conditions were taken from ground-based measurements from the Little Washita site on Day 193 of the Southern Great Plains 1997 (SGP97) experiment. The observations were interpolated to the four soil levels in the LSM. However, before using these as initial conditions for the LES-LSM runs, the soil model was run off-line for four complete diurnal cycles to allow the LSM to equilibrate. The noon time conditions after these four diurnal cycles were used as one set of initial soil conditions which we term *wet*. It is important to note that these *wet* initial conditions are such that the evaporation will be determined by a combination of the available soil moisture and the atmospheric demand rather than at the evaporative potential rate. *Dry* conditions were obtained similarly by running the LSM off-line for another seven diurnal cycles to allow the soil to dry under realistic forcing. Noon-time conditions after the one-week dry down period were chosen as *dry* conditions. Figure 1 shows the time-evolution of volumetric soil moisture and soil temperature for the four soil levels during the off-line LSM simulation. *Average* initial soil conditions were obtained by picking the noon-time soil conditions that provided surface fluxes nearly equal to the noon-time fluxes averaged every day over the entire one-week dry-down period.

4. Simulations

The coupled LES-LSM simulations employ (600,100,144) grid points in the (x,y,z) directions representing a (30,5,2.88) km domain. Constant spacing of (50,50,20) meters is maintained in each of the (x,y,z) directions.

A geostrophic wind of 0 ms^{-1} is imposed in both x and y directions, therefore the simulations are in the free-convection limit. The only forcing imposed on the system is specified through the incoming solar radiation, which is set to 700 Wm^{-2} and is constant in time for all cases.

For all of the simulations, the initial potential temperature is constant with height (300K) within the PBL; at 790m, a relatively strong capping inversion is imposed (3K/0.1km) for one hundred meters; above this inversion ($z > 890\text{m}$), the stratification is 3 K/km.

The simulations were performed using two different overlying atmospheres. The first set of cases was initialized with a relatively wet atmosphere (8 g kg^{-1}) in the PBL, dropping sharply to 1 g kg^{-1} at the initial inversion height (840m), therefore these are wet PBLs that are ‘Drying’. In the second set of cases, the atmosphere was initialized dry (1 g kg^{-1}) throughout the entire domain and are therefore dry PBLs that are ‘Wetting’.

For each overlying atmosphere, nine simulations were performed (for a total of eighteen). Three of these are

horizontally homogeneous cases with soil conditions that are *wet*, *dry*, and *average* respectively. The subsequent six cases are initialized with horizontally heterogeneous soil moisture conditions. The heterogeneity that is imposed occurs solely in the x -direction as a step-function change between *wet* and *dry* conditions. We define λ as the wavelength of one complete *wet* and *dry* cycle. The wavelengths vary as $\lambda = [2, 3, 5, 7.5, 15, 30]$ km. At initial times, the x -extent of a single patch ($\lambda/2$) ranges therefore from $1.2z_i$ to $17.8z_i$. The soil conditions are homogeneous in the y -direction.

For the three types of cases discussed in this manuscript (Homogeneous: *average*, Heterogeneous: $\lambda = 5 \text{ km}$ and $\lambda = 2 \text{ km}$), the results are normalized by a combination of the horizontally- and time-averaged convective velocity scale w_*^\dagger and mixing ratio scale Θ_*^\dagger . For the (Homogeneous, $\lambda = 5 \text{ km}$, $\lambda = 2 \text{ km}$) cases, average w_* is (2.50, 2.44, 2.44) ms^{-1} for the ‘Wetting’ case and (2.62, 2.56, 2.56) ms^{-1} for the ‘Drying’ case. Similarly, Θ_* is $(0.86, 1.22, 1.23) \times 10^{-3} \text{ kg kg}^{-1}$ and $(0.79, 1.12, 1.13) \times 10^{-3} \text{ kg kg}^{-1}$, respectively. Averages are obtained from ten volumes representing nearly 4.5 turnover times.

5. Results

In the PBL, coherent organized structures are largely responsible for the transport of atmospheric constituents (*e.g.*, Schmidt and Schumann, 1989). Different stability regimes tend to produce varying types of organized motions (*e.g.*, Khanna and Brasseur, 1998). Heterogeneous surface forcing also produces organized motions (*e.g.*, Shen and Leclerc, 1995). Of interest is how organized motions induced through heterogeneous surface forcing alter the mechanics of turbulent transport compared to coherent structures in a homogeneously forced PBL.

A method to isolate organized motions induced by the heterogeneity is to partition a particular variable into its ensemble averaged, phase-correlated, and background turbulent components following Hussain and Reynolds (1970). Any random signal can be decomposed into

$$f(x,y,z,t) = \langle f \rangle(z) + f''(x,y,z,t) \quad (1)$$

or,

$$f(x,y,z,t) = \langle f \rangle(z) + f_p(x,z) + f'(x,y,z,t) \quad (2)$$

The ensemble average $\langle f \rangle(z)$ results from averaging over all (x,y,t) . In this analysis, a conditional phase average

$\dagger w_* = (g/\theta_0 \langle w''\theta'' \rangle_{sf} \langle z_i \rangle)^{1/3}$ and $\Theta_* = \langle w''q'' \rangle_{sf}/w_*$.

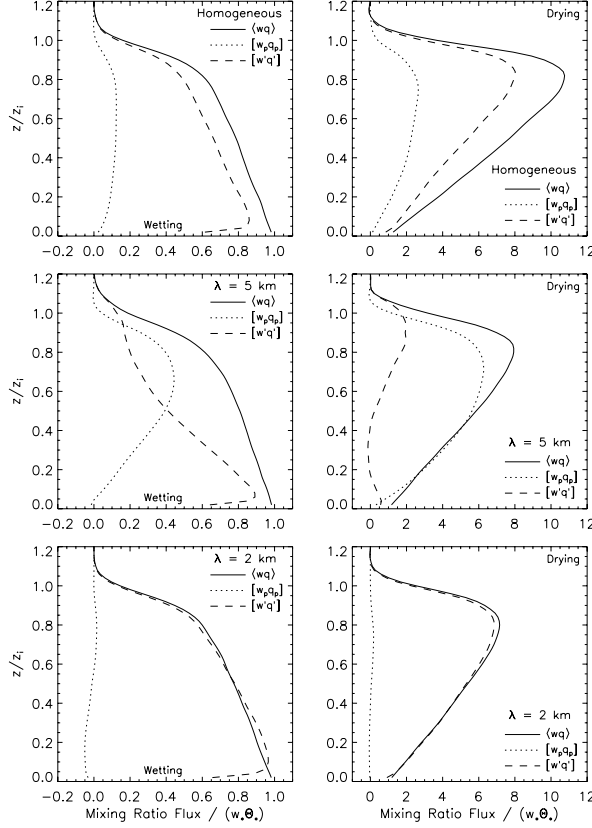


Figure 2: Vertical profiles of the total vertical mixing ratio flux $\langle wq \rangle$, the phase-correlated mixing ratio flux $[w_p q_p]$, and background turbulent mixing ratio flux $[w'q']$ for six cases. The left column are the wetting PBLs, and the right column are the drying PBLs. The top row are the *average* horizontally homogeneous cases, middle row are the $\lambda = 5$ km cases and the bottom row are the $\lambda = 2$ km cases.

$\tilde{f}(x, z)$ is defined as an average over (y, t) and also periodically imaged in x with length λ . For the homogeneous cases $\tilde{f}(x, z)$ is defined solely by an average over (y, t) . The phase-correlated component $f_p(x, z)$ is defined as $\langle f \rangle(z) - \tilde{f}(x, z)$. The streamwise average of the phase correlated component is written as $[f_p](z)$ and it should be noted that by construction, $[f_p](z) = 0$.

For the Homogeneous cases (top two panels of Figure 2), profiles of the total vertical mixing ratio flux exhibit expected behavior: in the wetting PBL, the flux is dominated by the surface flux while in the drying PBL the flux is dominated by entrainment of dry air from aloft. Counter to expectation, the phase-correlated component of the flux is non-zero. Since the conditions simulated here are freely convective ($z_i/L \rightarrow -\infty$), organized motions produced in the homogeneous cases tend to occur like Rayleigh-Bénard cells, otherwise known as thermals

or plumes (Khanna and Brasseur, 1998). We speculate that since these simulations are a fully coupled system, the development of a plume tends to be locked to a particular location due to the organized drying of land-surface beneath the plume. A check of lateral correlations suggests that the width of the box is sufficient that the periodic boundary conditions are not responsible for this result (not shown). Although the phase-correlated component is important, for both types of boundary layers, the turbulent component performs the majority of the vertical transport of water vapor mixing ratio with homogeneous surfaces.

In the presence of large scale heterogeneity, the character of organized motions in PBL flows is very different. Spatial contrast between regions of high and low soil moisture results in a varying partitioning of the incoming solar radiation between sensible, latent and soil heat fluxes. The partitioning is again affected by the overlying atmosphere being moist (dry) resulting in less (more) demand for moisture from the soil. In these simulations the horizontally- and time-averaged surface fluxes for both the wetting and drying PBLs are nearly equal for all λ . Roy and Avissar (2000) found that heterogeneity induces a horizontal pressure gradient and if that force is larger than the buoyant forcing, the atmosphere is dominated by ‘rolls’. If the balance switches such that the buoyant forcing dominates the pressure gradient, then the rolls are typically broken down by plumes.

The bottom four panels of Figure 2 show that even under heterogeneous surface forcing, profiles of vertical mixing ratio fluxes are nearly identical to those under homogeneous forcing. The peak near the entrainment zone in the Drying PBL cases is slightly smaller than the peak in the Homogeneous case, but this should be expected since the entrainment is a free parameter in the system and is therefore a result of the flow that develops. Of interest, however, is the variation in the partitioning between the components that make up the total vertical mixing ratio flux. The $\lambda = 5$ km heterogeneity induces ‘rolls’ as exhibited by an increase in the contribution from the phase-correlated component in both these cases. Figure 3 suggests that the ‘roll’ dynamics between these two $\lambda = 5$ km cases are nearly the same since $[w_p]$ increase similarly. Therefore, the difference seen between the ‘Wetting’ and ‘Drying’ PBLs is largely due to the difference in the moisture gradient across the entrainment interface. On the other hand, the phase-correlated component of the vertical mixing ratio flux is nearly zero for both $\lambda = 2$ km cases (Figure 2). Rayleigh-Bénard cells in the PBL typically have horizontal length scales of about 2.5 km (Roy and Avissar, 2000), therefore, the reduction of $[w_p]$ in these cases compared to the Homogeneous cases results largely from a competition between heterogeneity-induced organized motions and the

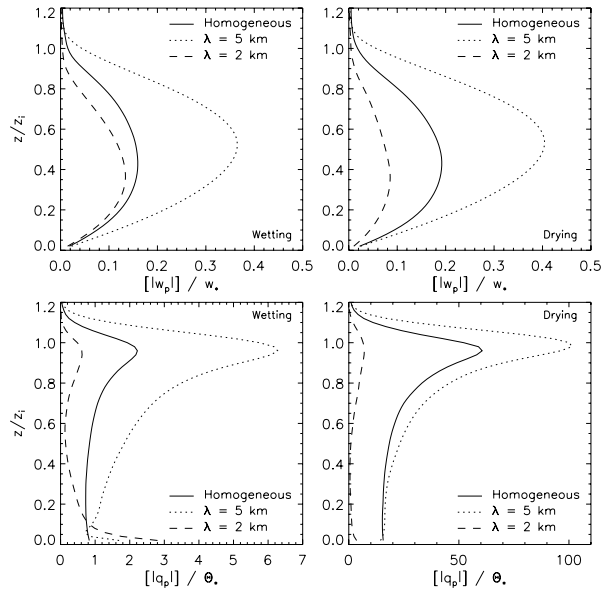


Figure 3: Vertical profiles of the x -average of the phase-correlated vertical velocity $[w_p]$ and mixing ratio $[q_p]$ for six cases. The left column are the wetting PBLs, and the right column are the drying PBLs.

Rayleigh-Bénard cells that are of nearly equal scale. Although $[w_p]$ is slightly reduced for these cases, Figure 3 suggests that the reduction in the phase-correlated component of the flux largely results from a destruction of the phase-correlated water vapor mixing ratio throughout the mid-PBL region where the phase-correlated vertical velocity is maximized.

Important implications from this analysis are that if a single point measurement occurs within regions of large-scale soil moisture heterogeneity and the heterogeneity-induced component of the total vertical mixing ratio flux is ignored, then the measurement will gravely misestimate the total flux. The direction and magnitude of error depends on the moisture gradient across the entrainment zone and on the scale of the heterogeneity.

6. Conclusions

Through coupled LES-LSM simulations of wetting and drying boundary layers, the influence of large-scale heterogeneity is shown to induce organized motions. The phase-correlated component can be either the sole contributor to the vertical water vapor mixing ratio flux or make zero contribution depending on the scale of the heterogeneity. Important findings are that if a researcher plans to use the eddy-correlation technique to measure vertical water vapor mixing ratio fluxes at a point within a region of large-scale moist or dry soil conditions, they

could dramatically misestimate the vertical fluxes if they ignore the contributions to the flux from organized motions induced via heterogeneous surface forcing. More detail and quantitative results will be presented in the talk.

Acknowledgements

NCAR is sponsored in part by the National Science Foundation. The majority of this work was supported by the NASA Land Surface Hydrology program through contract NAG5-8839. We thank Michael Ek for supplying us with the NOAA land surface model and for helpful discussions.

REFERENCES

- Chang, S., D. Hahn, C.-H. Yang, and D. Norquist, 1999: Validation of the CAPS model land surface scheme using the 1987 Cabauw/PILPS dataset, *J. Appl. Meteorol.*, **38**, 405–422.
- Garratt, J. R., 1993: Sensitivity of climate simulations to land-surface and atmospheric boundary-layer treatments - A review, *J. Clim.*, **419-449**, 349–377.
- Hussain, A. K. M. F. and W. C. Reynolds, 1970: The mechanics of an organized wave in turbulent shear flows, *J. Fluid Mech.*, **41**, 241–258.
- Khanna, S. and J. G. Brasseur, 1998: Three-dimensional buoyancy- and shear-induced local structure of the atmospheric boundary layer, *J. Atmos. Sci.*, **55**, 710–743.
- Rowntree, P. R. and J. Bolton, 1983: Simulation of the atmospheric response to soil moisture anomalies over Europe, *Quart. J. Roy. Meteorol. Soc.*, **109**, 501–526.
- Roy, S. B. and R. Avissar, 2000: Scales of response of the convective boundary layer to land-surface heterogeneity, *Geophys. Res. Lett.*, **27**, 533–536.
- Schmidt, H. and U. Schumann, 1989: Coherent structure of the convective boundary layer derived from large-eddy simulation, *J. Fluid Mech.*, **200**, 511–562.
- Shen, S. and M. Y. Leclerc, 1995: How large must surface inhomogeneities be before they influence the convective boundary layer structure? A case study, *Quart. J. Roy. Meteorol. Soc.*, **121**, 1209–1228.
- Sullivan, P. P., J. C. McWilliams, and C.-H. Moeng, 1996: A grid nesting method for large-eddy simulation of planetary boundary-layer flows, *Boundary-Layer Meteorol.*, **80**, 167–202.